JCI insight

T cells expressing chimeric antigen receptor promote immune tolerance

Antonio Pierini, … , Seung K. Kim, Everett H. Meyer

Research Article   Immunology   Transplantation

Cellular therapies based on permanent genetic modification of conventional T cells have emerged as a promising strategy for cancer. However, it remains unknown if modification of T cell subsets, such as Tregs, could be useful in other settings, such as allograft transplantation. Here, we use a modular system based on a chimeric antigen receptor (CAR) that binds covalently modified mAbs to control Treg activation in vivo. Transient expression of this mAb-directed CAR (mAbCAR) in Tregs permitted Treg targeting to specific tissue sites and mitigated allograft responses, such as graft-versus-host disease. mAbCAR Tregs targeted to MHC class I proteins on allografts prolonged islet allograft survival and also prolonged the survival of secondary skin grafts specifically matched to the original islet allograft. Thus, transient genetic modification to produce mAbCAR T cells led to durable immune modulation, suggesting therapeutic targeting strategies for controlling alloreactivity in settings such as organ or tissue transplantation.

Find the latest version:

https://jci.me/92865/pdf

T cells expressing chimeric antigen receptor promote immune tolerance

Antonio Pierini,[1,2] Bettina P. Iliopoulou,[1] Heshan Peiris,[3] Magdiel Pérez-Cruz,[1] Jeanette Baker,[1] Katie Hsu,[1] Xueying Gu,[3] Ping-Ping Zheng,[1] Tom Erkers,[1] Sai-Wen Tang,[1] William Strober,[1] Maite Alvarez,[1] Aaron Ring,[4] Andrea Velardi,[2] Robert S. Negrin,[1] Seung K. Kim,[3] and Everett H. Meyer[1]

[1]Division of Blood and Marrow Transplantation, Stanford University School of Medicine, Stanford, California, USA. [2]Department of Medicine, Hematopoietic Stem Cell Transplantation Program, University of Perugia, Perugia, Italy. [3]Department of Developmental Biology, Stanford University School of Medicine, Stanford, California, USA. [4]Department of Molecular and Cellular Physiology, Stanford University, Stanford, California, USA.

Cellular therapies based on permanent genetic modification of conventional T cells have emerged as a promising strategy for cancer. However, it remains unknown if modification of T cell subsets, such as Tregs, could be useful in other settings, such as allograft transplantation. Here, we use a modular system based on a chimeric antigen receptor (CAR) that binds covalently modified mAbs to control Treg activation in vivo. Transient expression of this mAb-directed CAR (mAbCAR) in Tregs permitted Treg targeting to specific tissue sites and mitigated allograft responses, such as graft-versus-host disease. mAbCAR Tregs targeted to MHC class I proteins on allografts prolonged islet allograft survival and also prolonged the survival of secondary skin grafts specifically matched to the original islet allograft. Thus, transient genetic modification to produce mAbCAR T cells led to durable immune modulation, suggesting therapeutic targeting strategies for controlling alloreactivity in settings such as organ or tissue transplantation.

Introduction

Recent advances with genetically modified T cells have led to promising cellular therapies, including engineering T cells to express chimeric antigen receptor (CAR) for cancer treatment (1, 2). Conventional T cells expressing surface CARs have been directed to specific selected antigens expressed by neoplastic cells, inducing antigen-mediated immune responses, such as tumor regression and elimination (3, 4). Using this approach, CAR T cells have emerged as a new therapy for several hematologic cancers and have ushered in a new era for CAR-based cancer immunotherapy (5–8).

Recently, CAR technology has also been investigated for modulating immune responses in non-neoplastic disease settings (9). CD4+CD25+FoxP3+ Tregs are a subpopulation of T cells that can suppress conventional CD4+ and CD8+ T cell (Tcon) proliferation, and the function of multiple other immune cell types, to govern physiological immune responses. Tregs have been engineered to express CARs, with the aim of suppressing antigen-specific immune responses in different diseases (10, 11). The use of Treg adoptive transfer in preclinical models and in human subjects has been effective in preventing graft-versus-host disease (GvHD), a life-threatening complication of hematopoietic stem cell transplantation involving donor cell–mediated immune attack of host tissues (4, 12–16). However, major challenges to the clinical implementation of Treg-based therapies remain. These include (a) a need for Treg targeting to tissue sites of immune attack, thereby limiting "off-target" effects; (b) a requirement for Treg activation to enhance their function; and (c) a need for expansion of functional Tregs, which constitute a relatively rare circulating population (15, 17–19).

Previous CAR T and Treg strategies have involved expression of an external targeting scFv antibody-binding domain fused with internal signaling domains of the costimulatory factors CD28 and CD3ζ. There is some evidence that CD28 costimulation of Tregs can modulate their activation, and recent studies suggest that CD28/CD3ζ internal stimulatory domains can enhance Treg function (20).

Here, we used transient T cell genetic engineering to permit expression of a CAR in Tcons and Tregs that bind antibodies conjugated in the Fc region with FITC (hereafter called "mAbCAR" T cells).

This permitted efficient modular use of previously characterized mAbs conjugated with FITC that (a) bound mAbCAR, (b) activated T cell function in vitro and in vivo, and (c) promoted homing of T cells expressing mAbCAR to specific antigens and cells. We used the mAbCAR approach in transplantation models to direct Tcon and Treg homing after adoptive transfer in order to modulate and control GvHD while maintaining graft-versus-tumor (GvT) effects. In mice, mAbCAR-expressing Tregs directed to MHC-mismatched pancreatic islet allografts prolonged allograft survival and elicited alloantigen-specific tolerance to secondary skin grafts. This work highlights the flexibility and the immune modulatory properties of mAbCAR Tregs in controlling alloreactivity and suggests these cells could be developed for translational purposes in T cell–based immunotherapies and tolerance induction.

Results

A flexible mAb-directed CAR to generate T cells and Tregs. To exploit the exquisite specificity of mAbs, we built a CAR that could be activated by binding to mAbs. To do this, we generated a CAR (clone 1X9Q) that specifically binds FITC, a standard mAb molecular conjugate. Briefly, we fused an anti-FITC scFv portion to murine CD28 and CD3ζ costimulatory domains and named this synthetic receptor "mAbCAR" (Figure 1, A and B). To facilitate detection of mAbCAR expression, we also incorporated the FLAG immunoepitope in mAbCAR (Figure 1A). CD28 is a costimulatory molecule widely tested in CAR T cell function (21, 22), with established roles in suppression by Tregs (20).

We used transient transfection to express the genomic DNA plasmid transgene encoding mAbCAR in primary T cells and Tregs. Transfection efficiency and surface expression kinetics were assessed by flow cytometric analysis by incubating FITC-conjugated isotype control mAb and an anti-FLAG mAb and quantifying FLAG$^+$ and FITC$^+$ cells. Both the whole T cell pool and Tregs expressed mAbCAR at efficiencies of approximately 30% (Figure 1, C and D). The level of FITC-conjugated antibody binding did not appear to depend on the specific antibody used (Figure 1, C and D). As expected, mAbCAR expression in T cells peaked and then was almost completely lost after approximately 3–4 days (Figure 1E).

mAbCAR T cell binding of FITC induces activation. To evaluate the activation of mAbCAR T cells by transfection and FITC binding, we purified mAbCAR T cells by flow cytometry and incubated these in vitro with different FITC-conjugated antibodies (KLH/G2a-1-1 or MECA-367) attached to a tissue culture well. Given that just the act of nucleofection and possibly other methods of transient transfection induced the activation of CD4$^+$ T cells, we assessed the expression of T cell activation markers by flow cytometry. We found that the transient transfection of the CAR construct with or without temporary incubation with FITC-conjugated mAb caused the same statistically significant upregulation of the activation marker CD69 as well as PD1 and LAG3 (Figure 2A, $P = 0.01$). Thus, in a very simplified in vitro system, mAbCAR T cells were nonspecifically activated in response to transfection and antibody coating. Further, using SPADE analysis after mass cytometry (23), we found that FITC-mediated activation was more pronounced in the effector memory subpopulations of both the observed CD4$^+$FoxP3^{neg} and CD4$^+$FoxP3$^+$ (Treg) mAbCAR T cells (Supplemental Figure 1; supplemental material available online with this article; https://doi.org/10.1172/jci.insight.92865DS1). After demonstrating that transfection and coating of FITC-conjugated mAb itself activates T cells equally independent of mAb used, we next evaluated how the specificity of mAbCAR T cells targeting influenced effector activity using FITC-conjugated mAb against MAdCAM1, a known cell-surface integrin mainly expressed in the endothelium of the gut and secondary lymphoid tissues, such as lymph nodes and spleen (24, 25). MAdCAM1 is also expressed by a small subset of primary splenocytes, and we used these as target cells for assaying MAdCAM1-mAbCAR T cells. We compared purified mAbCAR T cells incubated with FITC-conjugated MECA-367, a mAb specific for MAdCAM1, to T cells incubated with FITC-conjugated isotype control (KLH/G2a-1-1) mAb. After coculture of mAbCAR T cells with syngeneic C57BL/6 (H-2^b) mouse splenocytes that contain subsets of cells expressing the CAR construct with bound antibody targeted against MAdCAM1, we found that MAdCAM1-mAbCAR T cell activation, as quantified by expression of CD25 and CD69, was greater than activation of isotype-mAbCAR T cells (Figure 2B). Moreover, a higher percentage of MAdCAM1-mAbCAR T cells acquired an effector memory phenotype (CD44$^+$CD62L^{neg}, Figure 2, C and D). These findings suggest that activated mAbCAR T cells can be directed by mAbs that specifically bind cell surface antigen, and this interaction causes activation to persist in a complex in vitro system involving multiple splenocyte cell populations.

mAbCAR Tcon targeting directs T cell localization and modulates GvHD. T cell homing dynamics after adoptive transfer are critical for the development of GvHD, and tissue-specific T cells have been shown
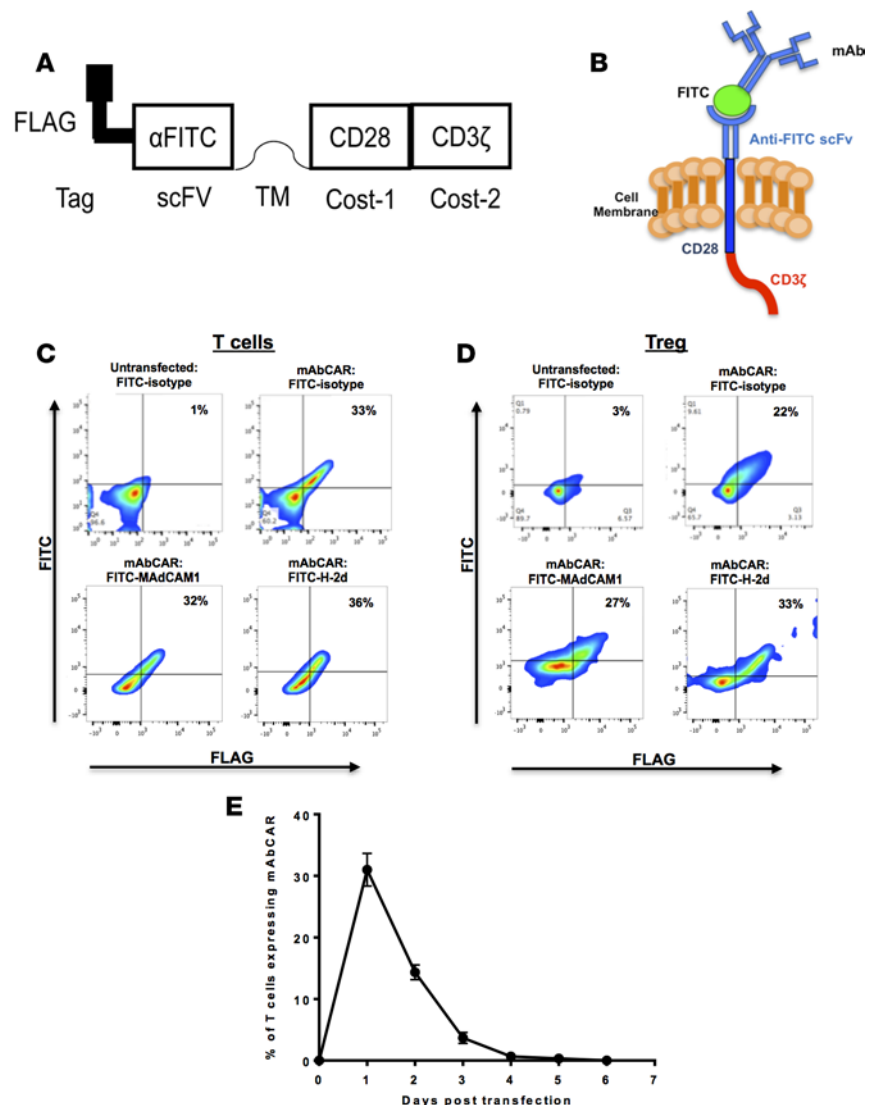
Figure 1. mAbCAR construct and its expression in transfected T cells and Tregs. (**A**) mAbCAR construct scheme. Schematic representation of mAbCAR construct expressing the anti-FITC scFv (1X9Q) and intramembrane CD28 and CD3ζ stimulatory domains. (**B**) mAbCAR protein model. Model of mAbCAR molecule expression by transfected T cells and loading with FITC-conjugated mAb. (**C**) mAbCAR expression in T cells. Representative flow cytometry plots of mAbCAR expression by untransfected or transfected T cells measured by anti-FLAG and different FITC-conjugated mAbs. (**D**) mAbCAR expression in Tregs. Representative flow cytometry plots of mAbCAR expression by untransfected or transfected Tregs measured by anti-FLAG and different FITC-conjugated mAbs. (**E**) mAbCAR expression over time. Kinetic of mAbCAR expression over time in T cells after transient transfection and incubation in vitro, assessed by flow cytometry Data derive from 1 of 3 consecutive experiments; mean ± SEM.

to play a crucial role in GvHD pathophysiology (26, 27). Thus, as an important initial test of our approach, we evaluated whether transient expression of our mAbCAR could durably influence T cell reconstitution after hematopoietic stem cell transplantation and mitigate GvHD severity. We hypothesized that targeting different cell surface antigens would produce distinct patterns of tissue localization by activated mAbCAR T cells, and we used in vivo bioluminescent imaging (BLI) after adoptive transfer to track luciferase-expressing (*luc*⁺) mAbCAR T cells. MAdCAM1 is expressed by the gut endothelium and has important roles in GvHD development and lethality (28, 29). By contrast, SDF1 (also known as CXCL12) is expressed in the bone marrow, spleen, and liver but not in the gut (30). Moreover, we did not detect expression of either MAdCAM1 or SDF1 on our mAbCAR T cells by flow cytometry. Thus, we evaluated mAbCAR T cells preincubated with anti-MAdCAM1 antibody or with anti-SDF1 antibody.
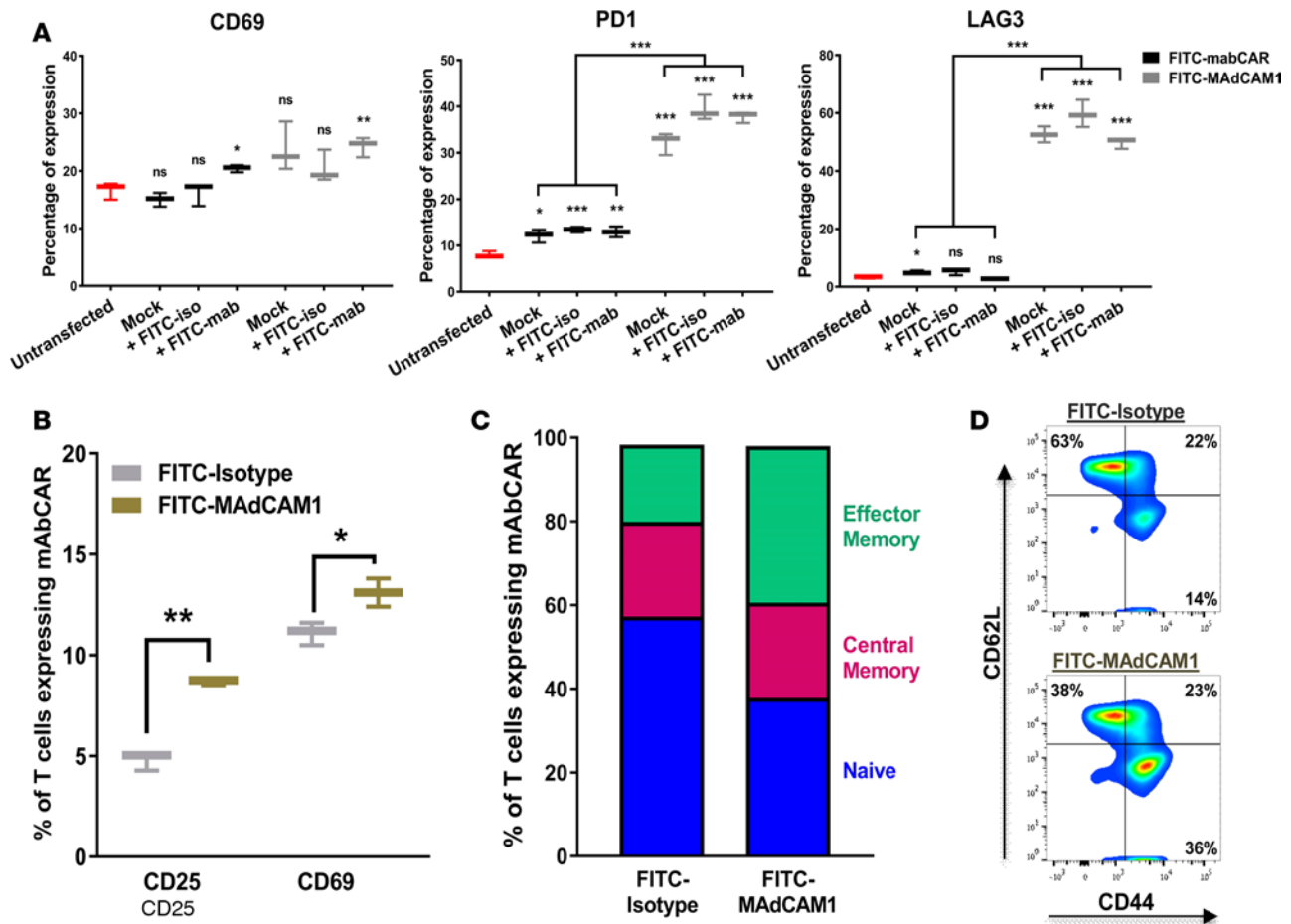
Figure 2. mAbCAR-expressing T cells are activated by FITC binding. (**A**) Analysis of mAbCAR-expressing CD4$^+$ T cells. Whiskers plots represent the percentage of surface expression of selected markers measured by flow cytometry (CD69, LAG3, PD1) before or after in vitro exposure to FITC (24 hours) in untransfected CD4$^+$ T cells (red), CD4$^+$ T cells that were mock transfected (black), and CD4$^+$ T cells that were transfected with mAbCAR construct (gray). Reported results derive from 3 independent experiments. Two-tailed Student's t test; mean ± SEM; *$P < 0.05$; **$P < 0.01$; ***$P < 0.001$. (**B**) Activation of mAbCAR T cells in vitro is target specific. mAbCAR T cells loaded with FITC-isotype control mAb or FITC-anti-MAdCAM1 mAb and cultured for 1 day with irradiated cell suspension derived from syngeneic spleen where MAdCAM1 was also expressed. CD25 and CD69 surface expression was measured by flow cytometry. Reported results derive from 3 independent experiments. Two-tailed Student's t test; mean ± SEM; *$P < 0.05$; **$P < 0.01$. (**C**) FITC mAbCAR does not modify T cell distribution. Percentage of naive (CD62L$^+$CD44^{neg}), central memory (CD62L$^+$CD44$^+$), and effector memory (CD62L^{neg}CD44$^+$) assessed by flow cytometry from mAbCAR T cells cultured as in **B**. Reported results derive from 3 independent experiments. Two-tailed Student's t test; mean ± SEM. (**D**) Representative flow cytometric plot of naive (CD62L$^+$CD44^{neg}), central memory (CD62L$^+$CD44$^+$), and effector memory (CD62L^{neg}CD44$^+$) in vitro–cultured FITC-isotype or FITC-MAdCAM1-mAbCAR T cells.

We adoptively transferred 1.0×10^6 cells MAdCAM1-mAbCAR or SDF1-mAbCAR T CD4$^+$ and CD8$^+$ Tcon- and T cell–depleted bone marrow (TCD BM) from C57BL/6 (H-2^b) donors into lethally irradiated allogeneic BALB/c (H-2^d) recipients. All the mice reached complete donor engraftment. Compared with untransfected control Tcons, in vivo imaging showed that MAdCAM1-mAbCAR Tcons had similar gut bioluminescence intensity. In contrast, SDF1-mAbCAR Tcons showed a distinct pattern of localization to other organs, including liver, spleen, and bone marrow (Figure 3, A and B). SDF1-mAbCAR Tcon recipient mice had significantly improved GvHD scores (Figure 3C) and weight profiles (data not shown, $P < 0.01$, Student's t test at days +7, +11, and +14 after transplant) compared with mice that received MAdCAM1-mAbCAR Tcons or control mice. Moreover, while there were lasting differences in clinical outcome between SDF-1– and MAdCAM1-directed Tcons, FACS analysis of mAbCAR Tcons reisolated after transfer showed that they almost completely lost mAbCAR expression and did not reveal detectable differences in production of surface homing molecules, such as CXCR4, CXCR5, CD62L or LPAM1, by CD4$^+$ and CD8$^+$ T cell subpopulations (Supplemental Figure 2). Together our findings suggest that specific antibodies and mAbCAR T cells can be used to direct T cell tissue localization after adoptive transfer to modulate GvHD outcomes.

In cancer therapeutics, GvT effects are an important therapeutic goal of adoptive T cell transfer, but it has been unclear whether GvT activity was affected in mAbCAR Tcons. To assess this, SDF1-mAbCAR Tcons or isotype-mAbCAR Tcons were transferred into transplanted allogeneic BALB/c mice that also received an intravenous infusion of *luc*+ A20 leukemia cells. Compared with control mice that received only A20 cells and died because of tumor progression, mice that received A20 cells and isotype-mAbCAR Tcons cleared the tumor but quickly died because of GvHD. Mice that received A20 cells and SDF1-mAbCAR Tcons cleared the tumor, had reduced GvHD, and had a better overall survival (Figure 3, D–F). Thus, mAbCAR Tcons coupled to FITC-anti-SDF1 antibody had reduced GvHD lethality while retaining GvT activity.

mAbCAR Tregs retain suppressive activity. To assess use of mAbCAR for Treg-based tolerance induction, we next tested if mAbCAR expression and mAb targeting could modulate natural CD4+CD25+FoxP3+ Treg activation and in vivo behavior. To evaluate the phenotype and immunoregulatory function of Tregs expressing mAbCAR, we evaluated both freshly isolated Tregs and Tregs expanded by in vitro culture (see Methods). Transient transfection and activation of mAbCAR Tregs with different FITC-conjugated antibodies in vitro did not significantly change FoxP3 expression (Figure 4A), and mAbCAR Tregs showed similar levels of phosphorylated STAT5 compared with control untransfected Tregs (Figure 4B). Likewise, we did not detect significant differences in T cell receptor (TCR) repertoires of the mAbCAR-transduced populations versus sham-transduced Treg populations (Figure 4C). Together, our findings suggest Tregs expressing mAbCAR retain hallmark Treg phenotypes.

We next evaluated if transfection and incubation with FITC-conjugated mAbs would activate Tregs. Using flow cytometry, we found that Tregs that expressed the mAbCAR construct alone and were coincubated with FITC-conjugated mAbs showed increased surface expression of the activation marker CD69 at 6 hours. While increased expression of CD69 persisted at 24 hours for mAbCAR Tregs without exposure to mAb, there was a statistically significant increase in CD69 expression in mAbCAR Tregs coincubated with FITC-conjugated mAb (Figure 4D). The same was observed for PD-1 expression but not LAG3 expression (Figure 4D). Activation of mAbCAR Tregs with FITC-conjugated antibodies in vitro led to significantly enhanced TCR-dependent proliferative responses following T cell activation in response to anti-CD3/CD28 beads (Figure 4E). The enhanced activation of Tregs was independent of the type of FITC-conjugated antibody used, indicating that our system could be used to investigate the effects of antibody binding specificity and targeting. These results also suggest that mAbCAR stimulation of Tregs does not induce anergy, but rather augments TCR-mediated expansion. Since polyclonal Tregs can activate in response to distinct allogeneic antigens and potentially become alloantigen specific, our findings are consistent with the possibility that mAbCAR stimulation could facilitate or rapidly accelerate the onset and persistence of alloantigen Treg recognition and activity.

To test if the enhanced capacity to activate and proliferate conferred by mAbCAR might alter the suppressive capacity of Tregs, we assayed Treg suppression of Tcon proliferation. As expected, Tregs suppressed the proliferation of Tcons (activated by anti-CD3/CD28 beads) in a dose-dependent manner. We observed that, while mAbCAR Tregs showed a slightly reduced suppressive capacity in comparison to untransfected Tregs when used at low Treg/Tcon ratios, regardless of the presence of FITC antibodies, all the different Treg groups exerted a strong suppressive effect on Tcon proliferation at all the tested ratios (Figure 4F).

To assess the suppressive capacity of mAbCAR Tregs in vivo, we adoptively transferred donor mAbCAR Tregs (exposed to FITC-MAdCAM1 antibody or FITC-isotype-control antibody) from C57BL/6 mice into lethally irradiated allogeneic BALB/c recipients prior to allogeneic donor Tcon and TCD BM. Both MAdCAM1- and isotype-mAbCAR Tregs were able to effectively prevent GvHD, and their efficacy was comparable to untransfected Tregs in terms of prolonged mouse survival (Figure 4G). Together, our findings confirm that cardinal Treg functions are maintained in mAbCAR Tregs and activated by FITC-conjugated antibodies.

Allogeneic islet tolerance induced by mAbCAR Tregs directed against islet alloantigen. Based on our findings, we postulated that mAbCAR could be used to target Tregs to transplanted allogeneic pancreatic islets and protect them from allograft rejection. We transplanted allogeneic *luc*+ pancreatic islets from BALB/c (H-2d) donors in the right subcapsular renal space of sublethally irradiated C57BL/6 albino (675 gray; H-2b) mice (Figure 5A). Donor islet survival was assessed by BLI and postmortem histology. To direct Treg function to transplanted islets, we transferred recipient-derived (H-2b) mAbCAR Tregs bound to mAbs directed against donor H-2Dd MHC-I antigen expressed only by donor BALB/c-derived islets (H-2Dd-mAbCAR Treg, Figure 5A). Compared with mice receiving isotype-mAbCAR Tregs or no Tregs after islet transplantation, mice that received H-2Dd-mAbCAR
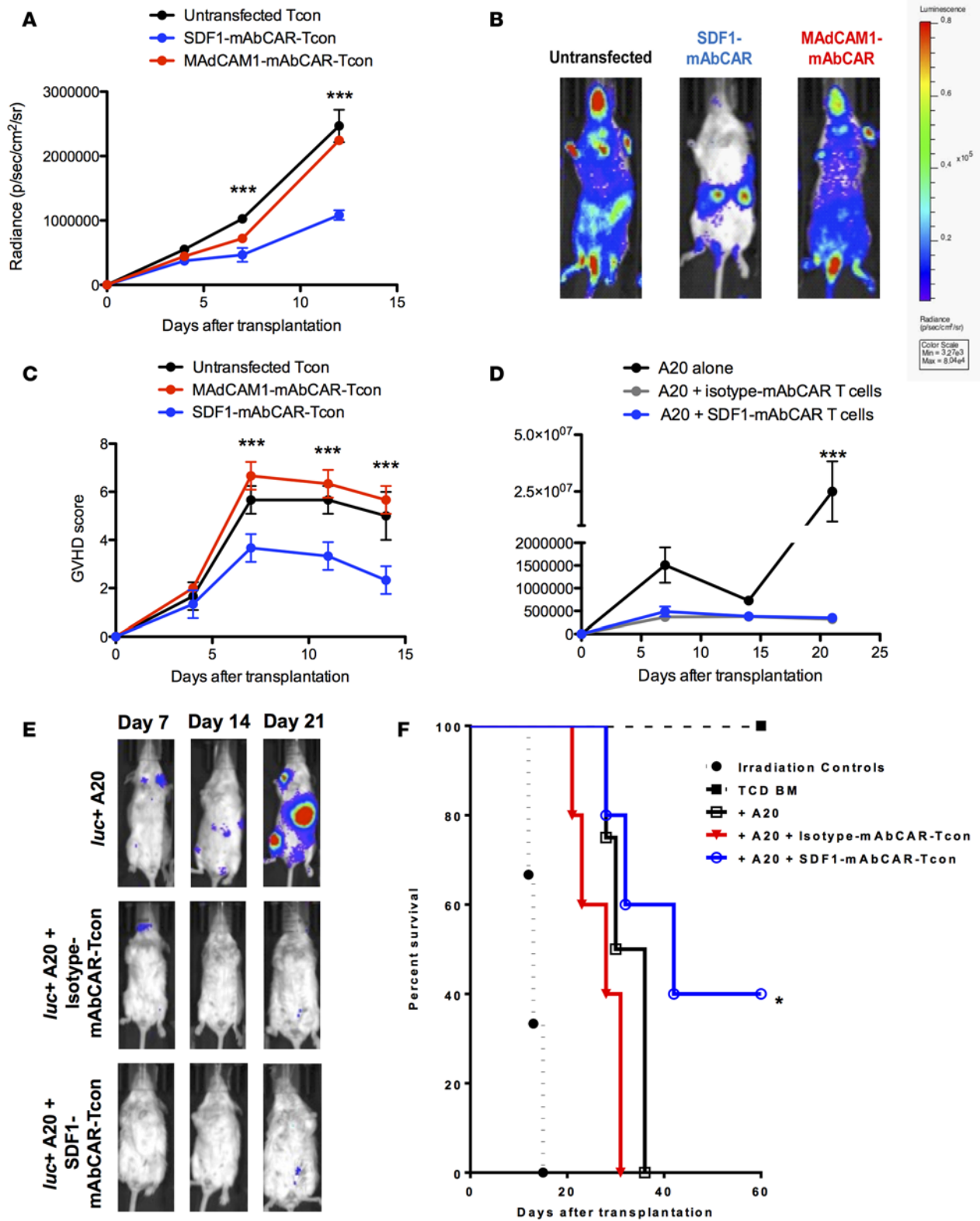
Figure 3. Tissue-specific FITC mAbs modulate mAbCAR T cell homing and function in vivo. (**A**) Targeting mAbCAR T cells regulates homing. The graph shows bioluminescent signal from allogeneic luc^+ untransfected Tcons (black), luc^+ SDF1-mAbCAR Tcons (blue), or luc^+ MAdCAM1-mAbCAR Tcons (red) at day +4, +7, and +12 after transfer in mice that received TCD BM at day 0. One representative of three consecutive experiments is presented; 2–4 mice/group were used in each experiment. ANOVA test with Bonferroni post-test; mean ± SEM; ***P < 0.001. (**B**) Targeting mAbCAR T cells alters localization. Representative bioluminescent images of mice that received luc^+ untransfected Tcons, luc^+ SDF1-mAbCAR Tcons, or luc^+ MAdCAM1-mAbCAR Tcons at day +12 after transfer. Data are representative of 1 of 3 consecutive experiments. (**C**) Targeting mAbCAR T cells modulates GvHD. GvHD score over time of recipient mice that received allogeneic untransfected Tcons, SDF1-mAbCAR Tcons, or MAdCAM1-mAbCAR Tcons. One representative of three independent experiments is presented. ANOVA test with Bonferroni post-test; mean ± SEM; ***P < 0.001. (**D**) mAbCAR T cells mediate graft-versus-tumor effects. Tumor growth analyzed by BLI in lethally irradiated BALB/c mice that received allogeneic C57BL/6 TCD BM and luc^+ A20 alone (black), luc^+ A20 and allogeneic isotype-mAbCAR Tcons (gray), or luc^+ A20 and allogeneic SDF1-mAbCAR Tcons (blue). One representative of two consecutive experiments is reported; at least 3 mice/group were used. Two-tailed Student's t test; mean ± SEM; ***P < 0.001. (**E**) mAbCAR T cells eliminate tumor in vivo. Representative bioluminescent images of lethally irradiated BALB/c mice that received allogeneic C57BL/6 TCD BM and luc^+ A20 alone, luc^+ A20 and isotype-mAbCAR Tcons, or luc^+ A20 and SDF1-mAbCAR Tcons at day +7, +14, and +21 after transplant. One representative of two consecutive experiments is reported; at least 3 mice/group were used. (**F**) SDF1-directed mAbCAR T cells enhance survival. Survival of lethally irradiated BALB/c mice that received irradiation alone (black circle), allogeneic C57BL/6 TCD BM (black squares), TCD BM + luc^+ A20 alone (white squares in black), TCD BM + luc^+ A20 + allogeneic isotype-mAbCAR Tcons (red triangles), TCD BM + luc^+ A20 + allogeneic SDF1-mAbCAR Tcons (white circles in blue). One representative of two consecutive experiments is reported; at least 3 mice/group were used. Log-rank survival test; *P < 0.05 for differences between the groups that received luc^+ A20 alone and luc^+ A20 + allogeneic SDF1-mAbCAR Tcons.

Tregs showed significantly enhanced islet survival (P = 0.002; Figure 5, B and C). FACS analysis of cell suspensions obtained from reisolated renal islet grafts showed reduction in host-type CD8$^+$ T cell infiltration in the presence of FITC-H-2D^d-mAbCAR Tregs at day +10 after islet transplantation (Figure 5D). Thus, mAbCAR Tregs directed to allogeneic islet grafts can significantly improve allograft survival (Figure 5E).

H-2D^d-mAbCAR-directed Tregs localize in proximity to allogeneic pancreatic islet grafts. To demonstrate localization by H-2D^d-mAbCAR Tregs to islet allografts, we used islets from donor wild-type BALB/c animals and mAbCAR Tregs from recipient C57BL/6 mice that express both luciferase and GFP$^+$. BLI revealed that the bioluminescent signal intensity of H-2D^d-mAbCAR Tregs was significantly greater compared with isotype-control mAbCAR Tregs (Figure 6, A and B). Ex vivo BLI of the isolated right kidney at day +10 after islet graft transplantation confirmed greater signal in kidneys from mice that received allogeneic islets and H-2D^d-mAbCAR Tregs (Supplemental Figure 3).

Histological analysis confirmed the presence of GFP$^+$ H-2D^d-mAbCAR Tregs adjacent to or within transplanted islets that were clearly detectable in the kidney capsule of mice that received mAbCAR Treg treatment at day +10 after adoptive transfer, indicating an increased ability to home in selected target tissues (Figure 6, C and D). H-2D^d-mAbCAR Treg expansion was also detectable in secondary lymphoid organs of the same animals (Figure 6E). In evaluation of splenocytes at day +10 after islet transplantation and adoptive transfer of H-2D^d-mAbCAR Tregs, we found that Tregs showed a trend toward an increased expression of markers, such as CD69 and CD25, consistent with a highly activated status (Figure 6F). However, as expected, FLAG immunoepitope expression by Tregs was undetectable by immunostaining, confirming loss of expression of the original FLAG-tagged mAbCAR construct. Thus, Tregs unexpectedly localized to allografted islets long after transduced Tregs lost mAbCAR expression (see Figure 1E). Thus, despite transient mAbCAR expression, we observed evidence of prolonged mAbCAR Treg localization and suppressive Treg function.

mAbCAR Tregs acquire antigen specificity after adoptive transfer in vivo. Based on observations here of (a) durable peripheral tolerance to allogeneic islets after mAbCAR Treg transfer and (b) proliferation of mAbCAR Tregs upon TCR stimulation, we hypothesized that H-2D^d-mAbCAR Tregs might foster antigen-specific peripheral tolerance of tissue allografts by Tregs. To test this, we evaluated survival of secondary skin grafts, a rigorous assay of peripheral tolerance in this setting. Specifically, we grafted skin on C57BL/6 albino mice 30 days after they had received allogeneic BALB/c islets and recipient-derived H-2D^d-mAbCAR Tregs or BALB/c islets and isotype-control mAbCAR Tregs. Each albino C57BL/6 recipient mouse then received two skin grafts, one from an allogeneic BALB/c moue (that was H-2D^d, MHC matched with the previous islets) and one from allogeneic FVB/n mice (not MHC matched with the previous islets and therefore "third party"). Mice that previously received isotype-mAbCAR Tregs showed quick rejection of both the skin grafts, but mice that were infused with H-2D^d-mAbCAR Tregs showed a statistically significant prolonged survival of only the MHC-matched BALB/c-derived skin grafts, measured in a blinded fashion (Figure 7). Histology of the skin grafts at 2 weeks after skin transplantation showed the MHC-matched BALB/c grafts that lacked detectable signs of rejection compared with the "third-party" grafts (Supplemental Figure 4). These data further demonstrate that H-2D^d-mAbCAR Tregs acquired antigen-specific suppressive function, even though mAbCAR expression was transient. Moreover to confirm such results
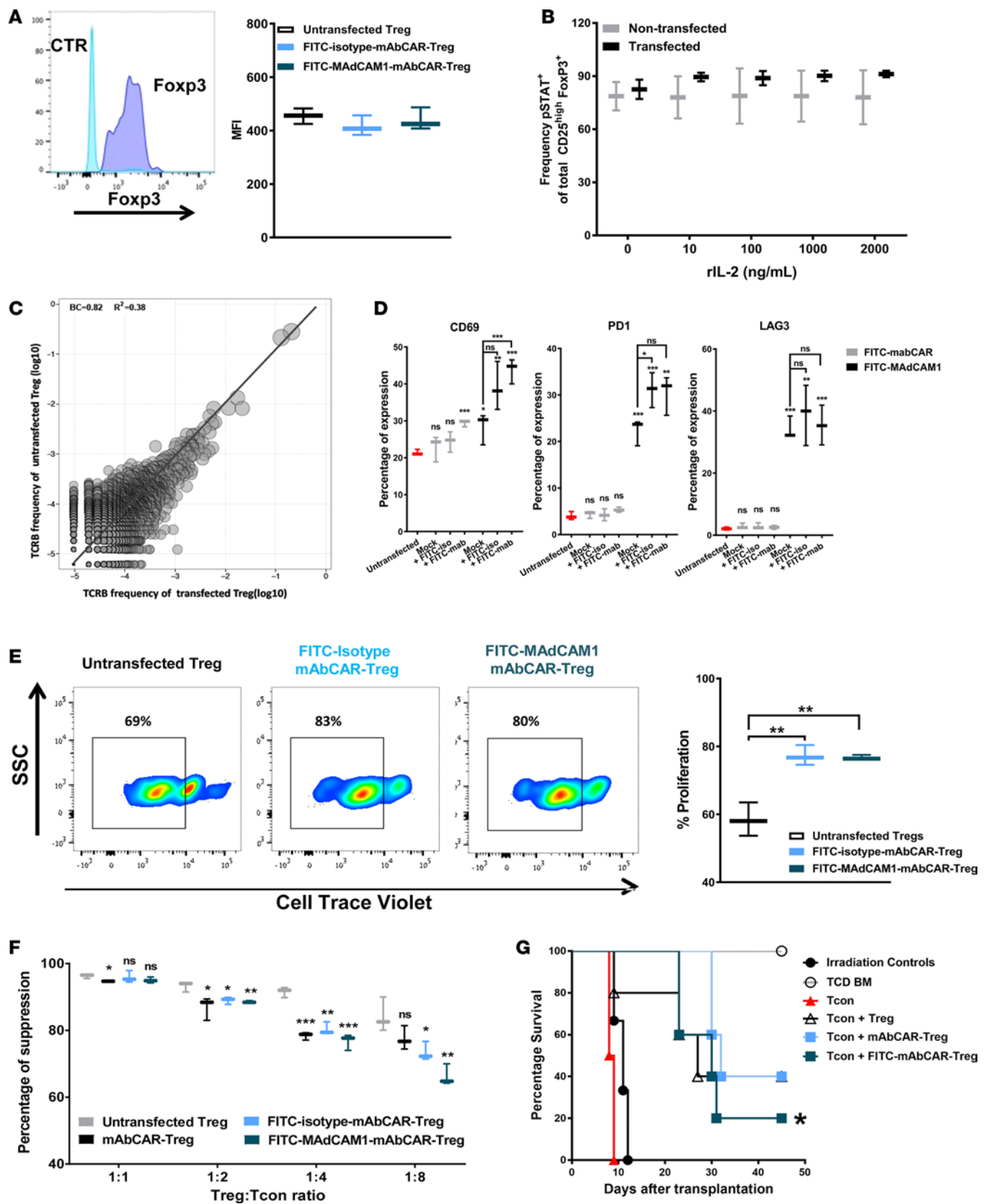
Figure 4. mAbCAR Tregs retain phenotype and function. (**A**) mAbCAR Tregs retain FoxP3 expression. Histograms of sample FoxP3 staining (dark blue) in comparison to isotype control (light blue) of FoxP3+ selected Tregs. FoxP3 intranuclear expression in untransfected Tregs, FITC-isotype-mAbCAR Tregs, and FITC-MAdCAM1-mAbCAR Tregs. Mean fluorescence intensity (MFI) of 1 representative of 3 consecutive experiments is reported. (**B**) mAbCAR Tregs retain STAT5 phosphorylation. Frequency of phosphorylated STAT5 expression in untransfected and transfected Tregs. One representative of two consecutive experiments is reported. (**C**) mAbCAR Treg TCRβ repertoire is unchanged. The TCRβ CDR3 clone frequency was obtained by TCR nucleotide sequencing. Pearson correlation between untransfected and transfected Tregs is r = 0.92, $P < 2.2^{-16}$. One representative of two consecutive experiments is reported. (**D**) Exposure to FITC-coupled antibodies activates mAbCAR Tregs. Whiskers plots represent percentage of expression of selected markers (CD69, LAG3, PD1) before or after in vitro exposure to FITC (24 hours) in mAbCAR Tregs. Data show marker expression in untransfected Tregs (red), mock transfected Tregs (black), and mAbCAR Tregs (gray). n = 2 independent experiments. (**E**) FITC mAbCAR expression and antibody binding increase Treg proliferation. Percentage of proliferation of untransfected Tregs, FITC-isotype-mAbCAR Tregs, and FITC-MAdCAM1-mAbCAR Tregs after culture with anti-CD3/CD28 beads, measured through cell trace violet dilution. Sample FACS analysis is also shown. One representative of two consecutive experiments is reported. (**F**) mAbCAR Tregs suppress activated T cells in vitro. Percentage of suppression of T cell proliferation by untransfected Tregs, mAbCAR Tregs, FITC-isotype-mAbCAR Tregs, and FITC-MAdCAM1-mAbCAR Tregs after 4 days stimulation with irradiated allogeneic splenocytes at T cell/Treg ratios of 1:1, 1:2, 1:4, and 1:8, measured through cell trace violet analysis. One representative of two consecutive experiments is reported. (**G**) mAbCAR Tregs prevent GVHD in vivo. Survival of lethally irradiated BALB/c mice that received allogeneic irradiation alone, TCD BM alone, TCD BM + Tcons, TCD BM + Tcons + untransfected Tregs, TCD BM + Tcons + mAbCAR Tregs, and TCD BM + Tcons + FITC-isotype-mAbCAR Tregs. One representative of three consecutive experiments is reported; at least 3 mice/group were used. Log-rank survival test; for differences between TCD BM + Tcons versus TCD BM + Tcons + untransfected Tregs or TCD BM + Tcons + mAbCAR Tregs or TCD BM + Tcons + FITC-isotype-mAbCAR Tregs. (**A**, **B**, and **D**–**F**) Two-tailed Student's t test; mean ± SEM; *P < 0.05; **P < 0.01; ***P < 0.001.

and to better understand if FITC-H-2D^d mAb–mediated binding is responsible for H-2D^d-mAbCAR Treg antigen specificity, we stimulated the proliferation of these cells with irradiated splenocytes derived from C57BL/6 mice (H-2^b) MHC matched with the Tregs, BALB/c mice (H-2^d) that represent a target for FITC-H-2D^d mAb, and FVB/N mice (H-2^q) that were third party. We observed that, even in this in vitro environment, H-2D^d-mAbCAR Tregs increased their proliferative ability only when exposed to targeted irradiated splenocytes (Supplemental Figure 5). Together, our data strongly suggest that mAbCAR and similar approaches could be used to promote, target, and enhance Treg function and peripheral immune tolerance induction, with striking improvements in tissue or organ allograft survival.

Discussion

The genetic modification of T cells to direct their activation to specific targets in vivo has become a successful strategy for cancer immunotherapy, but relatively less is known about how adoptive transfer of activated CAR T cells or Tregs might influence the recipient immune system in clinical settings such as GvHD or allotransplant tolerance. For example, while studies suggest that human Tregs could be effectively converted to CAR Tregs to target allogeneic cells that express HLA-A2 (12, 31, 32) very little is yet known about how CAR Tregs might alter immune responses or their interplay with antigen-specific tolerance. In one study, the adoptive transfer into mice of human CAR Tregs targeted to factor VIII reduced immune reactivity against factor VIII, even after adoptively human CAR Tregs were cleared by the recipient murine immune system. This might suggest that a transient intervention with CAR Tregs could have lasting antigen-specific suppression (27). To address these questions, we developed a system for expressing a CAR (mAbCAR) that binds to FITC and activates Treg functions, enabling flexible, modular targeting. Based on reliable, covalent coupling of FITC to mAbs, we tested and identified multiple antibodies that permitted *both* targeting and activation of T cells and Tregs. A similar approach was recently reported by Tamada et al. (33) and Ma et al. (34) to potentiate anticancer effects of T cells (35, 36).

Here, we used multiple systems to demonstrate that the introduction and transient expression of a CAR construct in adoptively transferred Tcons or Tregs permitted remarkable experimental control of T cell localization and activity. This improved outcomes of experimental disease models in mice, including GvHD, GvT effect, and tissue allograft tolerance. For example, expression of the mAbCAR construct that directed T cell activation modulated the severity of GvHD. mAbCAR Tregs maintain their suppressive phenotype and function (Figure 4), including suppression of Tcon proliferation both in vitro and in vivo. Mice that received CAR T cells directed to activate at the site of the gut (MAdCAM1) showed lethal gut GvHD, while those that received CAR T cells directed to activate mainly within the bone marrow compartment (SDF1) showed less GvHD, without impairing GvT responses or bone marrow engraftment. Thus, directing in vivo–infused Tcons away from GvHD targets (e.g., gut mucosa) results in reduced GvHD lethality. It is striking that transient transfection of a fraction of donor T cells could have a lasting effect on T cell reconstitution and GvHD; this suggests possible ways forward for T cell engineering in hematopoietic cell transplantation paradigms.
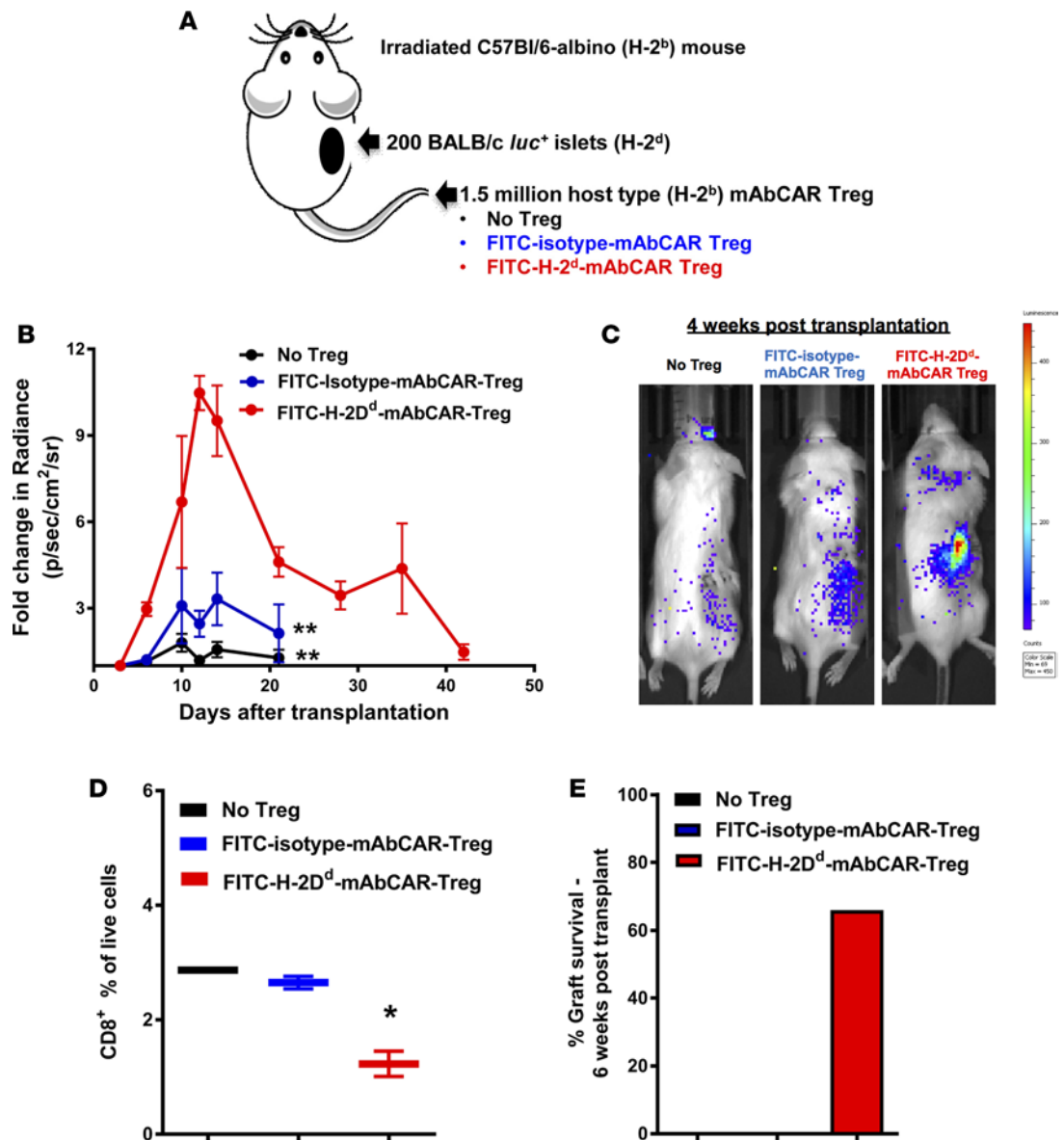
Figure 5. FITC-H-2Dᵈ-mAbCAR Tregs induce tolerance to allogeneic pancreatic islet grafts if directed against the islet MHC-I alloantigen. (**A**) Experimental scheme. Recipient C57BL/6 mice were conditioned with low-dose total body irradiation, followed by allogeneic islet cell transplantation of BALB/c donor islets under the right kidney subcapsule. On the same day of transplant, recipient mice also received sham or mAbCAR Tregs either coated with FITC-conjugated isotype or a mAb against H-2Dᵈ expressed by BALB/c tissue. (**B**) FITC-H-2Dᵈ-mAbCAR Tregs cause enhanced protection of islet allografts. Fold change over time of BLI uptake (radiance) from mice that received *luc*⁺ pancreatic islet graft alone (black circles), *luc*⁺ pancreatic islet graft + FITC-isotype-mAbCAR Tregs (blue circles), and *luc*⁺ pancreatic islet graft + FITC-H-2Dᵈ-mAbCAR Tregs (red circles). Values of fold change in BLI uptake below 1 have been censored. Data are pooled from 2 consecutive experiments; at least 2 mice per group were used in each experiment. ANOVA test with Bonferroni post-test; mean ± SEM; **$P < 0.001$ is reported for differences between the group that received *luc*⁺ pancreatic islet graft + FITC-H-2Dᵈ-mAbCAR Tregs versus the group that received *luc*⁺ pancreatic islet graft alone or *luc*⁺ pancreatic islet graft + FITC-isotype-mAbCAR Tregs. (**C**) BLI reveals in vivo persistence of pancreatic islet allografts after FITC-H-2Dᵈ-mAbCAR Treg transfer. Representative bioluminescent images of *luc*⁺ pancreatic islets at 4 weeks after islet transplant. (**D**) Mice receiving FITC-H-2Dᵈ-mAbCAR Tregs show reduced CD8⁺ T cell infiltrate in islet allografts. Percentage of pancreatic islet graft infiltration by host-type CD8⁺ T cells in mice that received no Treg treatment (black), FITC-isotype-mAbCAR Tregs (blue), FITC-H-2Dᵈ-mAbCAR Tregs (red) at 10 days after transplant. Data are representative of 1 of 2 consecutive experiments. Two-tailed Student's *t* test; mean ± SEM; *$P < 0.05$. (**E**) FITC-H-2Dᵈ-mAbCAR Tregs allow for prolonged survival of pancreatic islet allografts. Percentage of pancreatic islet graft survival at 6 weeks after transplant in mice that received no Treg treatment (black), FITC-isotype-mAbCAR Tregs (blue), and FITC-H-2Dᵈ-mAbCAR Tregs (red). Data are pooled from 2 consecutive experiments.
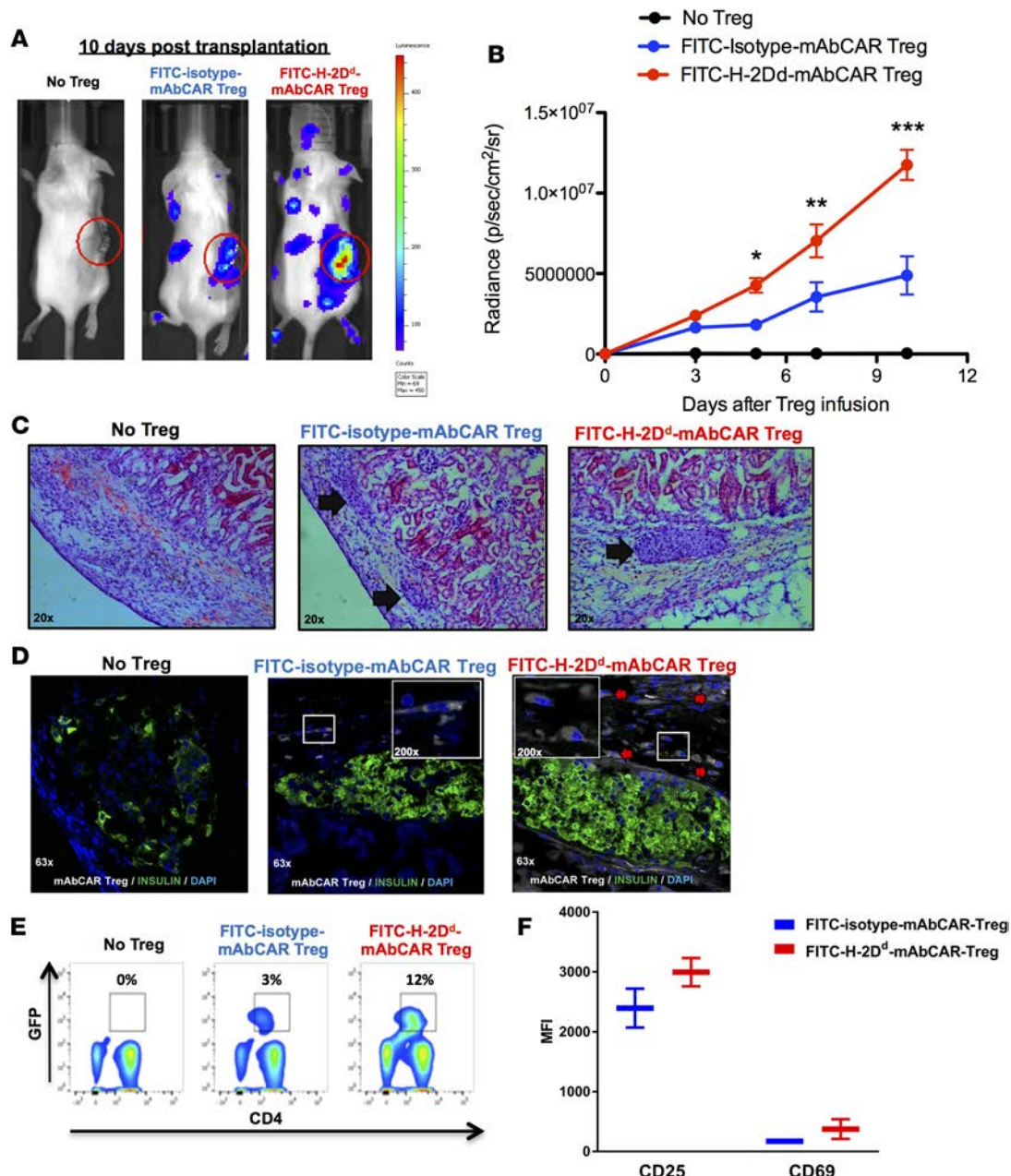
Figure 6. FITC-H-2Dᵈ-mAbCAR Tregs home and expand in proximity to allogeneic pancreatic islet grafts. (**A**) FITC-H-2Dᵈ-mAbCAR Tregs show enhanced localization to the islet allograft. Representative BLI images of sublethally irradiated mice that received a graft of allogeneic pancreatic islets alone, pancreatic islets + *luc*⁺ FITC-isotype-mAbCAR Tregs, and pancreatic islets + *luc*⁺ FITC-H-2Dᵈ-mAbCAR Tregs at day 10 after adoptive transfer. Data are representative of 1 of 3 consecutive experiments. (**B**) BLI-based quantification of FITC-H-2Dᵈ-mAbCAR Tregs in proximity of the graft. The graph represents BLI signal from standardized regions of interest in left kidney area (graft site) in sublethally irradiated mice that received a graft of allogeneic pancreatic islets alone (black), pancreatic islets + *luc*⁺ FITC-isotype-mAbCAR Tregs (blue), and pancreatic islets + *luc*⁺ FITC-H-2Dᵈ-mAbCAR Tregs (red) at day 3, 5, 7 and 10 after adoptive transfer. Data are representative of 1 of 3 consecutive experiments; at least 5 mice per group were used. ANOVA test with Bonferroni post-test; mean ± SEM; *$P < 0.05$; **$P < 0.01$; ***$P < 0.001$. (**C**) Mice receiving FITC-H-2Dᵈ-mAbCAR Tregs show improved islet allografts. Representative hematoxylin and eosin–stained histologic sections of allogeneic pancreatic grafts in mice that received no Treg treatment, GFP⁺-FITC-isotype-mAbCAR Tregs, or GFP⁺-FITC-H-2Dᵈ-mAbCAR Tregs 10 days after transplantation and Treg transfer (arrows = pancreatic islets under the kidney capsule). Original magnification, ×20. (**D**) FITC-H-2Dᵈ-mAbCAR Treg localization in proximity of the grafts. Confocal microscopy analysis demonstrates presence of transferred Tregs (GFP⁺, white, red arrows) in proximity of islet grafts (insulin, green) only in mice that received GFP⁺-FITC-H-2Dᵈ-mAbCAR Tregs. Data are representative of 1 of 3 consecutive experiments; at least 5 mice/group were used. Original magnification, ×63; ×200 (insets). (**E**) Mice receiving FITC-H-2Dᵈ-mAbCAR Tregs show increased Treg numbers. Percentage of transferred GFP⁺ Tregs in spleens of mice that received no Treg treatment, FITC-isotype-mAbCAR Tregs, and FITC-H-2Dᵈ-mAbCAR Tregs at 10 days after transplant. Data are representative of 1 of 2 consecutive experiments; at least 4 mice per group were used. (**F**) Mice receiving FITC-H-2Dᵈ-mAbCAR Tregs show increased Treg activation. Expression of CD25 and CD69 was assessed by flow cytometry in previously transferred GFP⁺ Tregs reisolated from spleens of mice that received FITC-isotype-mAbCAR Tregs (blue) or FITC-H-2Dᵈ-mAbCAR Tregs (red) at 10 days after transplant. Data are representative of 1 of 2 consecutive experiments; at least 4 mice/group were used.
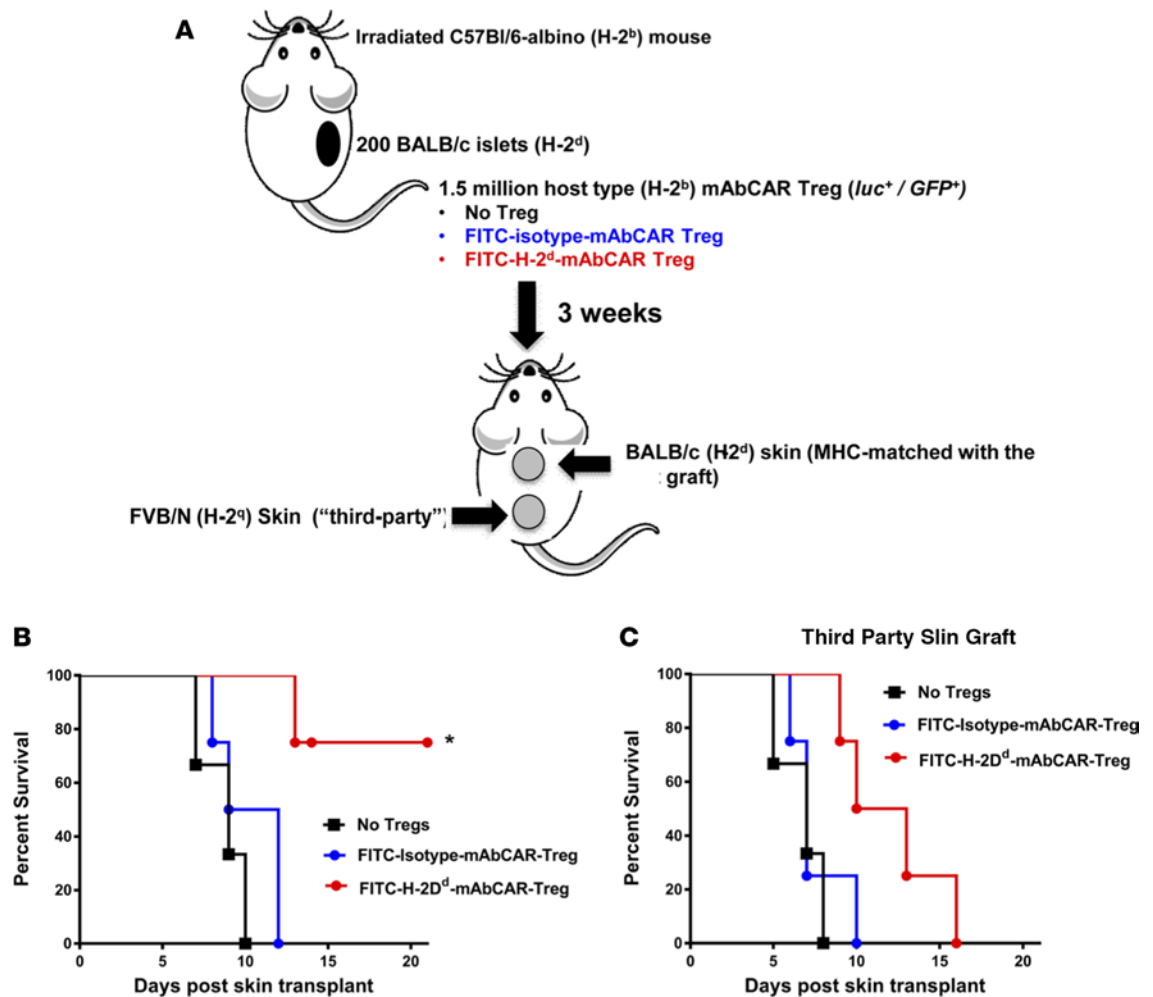
Figure 7. FITC-H-2D^d-mAbCAR Tregs acquire antigen specificity after in vivo transfer. (A) Experimental scheme. Mice that were previously transplanted with allogeneic pancreatic islet graft in the left kidney capsule received a secondary double skin graft MHC matched with the previously transplanted pancreatic graft (upper grafts) or "third party" (lower grafts). Data are representative of 2 consecutive experiments; at least 4 mice/group were used. Skins have been also transplanted in inverted position ("third-party" skins as upper grafts and MHC-matched skins as lower graft) in order to avoid technical bias. **(B)** Mice treated with FITC-H-2D^d-mAbCAR Tregs show alloantigen-specific protection of matched skin grafts. Survival of the skin graft that was MHC matched with the previously transplanted allogeneic islet graft in mice that received no Treg treatment (black squares), or FITC-isotype-mAbCAR Tregs (blue squares), or FITC-H-2D^d-mAbCAR Tregs (red squares). Log-rank survival test; *P < 0.05 is reported for differences between the group that received FITC-H-2D^d-mAbCAR Tregs versus the group that received no Treg treatment or FITC-isotype-mAbCAR Tregs. **(C)** FITC-H-2D^d-mAbCAR Tregs do not protect "third-party" skin grafts. Survival of the skin graft that was "third-party" with the previously transplanted allogeneic islet graft and the infused Tregs in mice that received no Treg treatment (black squares), or FITC-isotype-mAbCAR Tregs (blue squares), or FITC-H-2D^d-mAbCAR Tregs (red squares). Log-rank survival test; no statistical significance was detected between the three groups.

GvHD was not completely abrogated by the infusion of transiently transfected mAbCAR T cells directed against SDF1. We speculate that this reflects that (a) not every T cell was transfected and (b) some transfected T cells might circulate to other sites losing expression of mAbCAR. It will be useful to test if transfer of purified mAbCAR Tregs could further potentiate mAbCAR Treg ability to suppress gut GvHD.

In preclinical GvHD models, adoptive transfer of polyclonal CD25$^+$ Tregs has been associated with improved antigen-specific tolerance (37, 38), but these models depend upon impractically high doses of Tregs that have yet to be achieved in human translational science. Moreover, evidence is lacking from clinical trials that improved antigen-specific tolerance may result from Treg transfer. Immunotherapy with polyclonal Tregs has multiple challenges, including (a) a lack of mechanisms to "target" cells to sites of inflammation, (b) inactivation of suppressive functions and possible conversion to proinflammatory cells at

these sites, and (c) short-lived antigen-specific immune protection (15). Our studies provide evidence that genetically modified CAR Tregs could be used to overcome each of these problems. Our findings also raise the possibility that additional regulatory immune cell populations, including invariant natural killer T cells (39), Tr1 cells (40), and others, could be used in mAbCAR-based approaches.

While the use of transient transfected T cells has been explored in preclinical models and early-phase clinical trials, there is a lack of comprehensive reporting of the activation of T cells by the methodology of cell transduction or possibly by tonic background activation by the CAR internal stimulatory domain. As others have already shown (41), we observed that transient transfection of Tcons can activate T cells for 6–24 hours at least, and we report that this is true for Tregs as well. Interestingly, at 24 hours, our mAbCAR Tregs responding to FITC-conjugated mAb showed greater expression of CD69. This suggests that differences in the underlying biology of Tregs would cause them to respond to or depend upon CAR stimulation differently than Tcons.

To evaluate the use of CAR Tregs in islet transplantation, we investigated the effect of transient expression of CAR in Tregs directed to MHC mismatch in islet allografts. In clinical settings, such as leukemia, the relentless growth of target cells justifies use of stably transduced CAR T cells. However, we postulated that stable transduction using viral vectors or other strategies may not be practical for immunomodulation in settings, such as allograft tolerance. For example, polyclonal Treg subsets could become persistently activated and too immunosuppressive. Surprisingly, we found that Treg localization and allograft tolerance persisted long after the transient expression of the CAR construct. Even more remarkably, the one-time introduction of transiently expressing CAR Tregs resulted in antigen-specific peripheral tolerance, as MHC-matched secondary skin grafts were accepted, while "third-party" grafts were rejected. These results are particularly relevant, as they were observed in mice that received a skin graft 3 weeks after the previous islet transplant when Treg expansion had already occurred and when Tregs had completely lost the mAbCAR expression. Therefore, mAbCAR-mediated transient binding induces antigen specificity that persists, even if the initiating mAbCAR function itself is lost. H-2D^d-mAbCAR Tregs did not protect "third-party" grafts from rejection, but they tended to prolong their survival ($P > 0.05$, Figure 7C), possibly because of the efficient in vivo Treg expansion that occurred in this setting over time (Figure 6, A and B). Our findings suggest that transient transfection of Tregs might be useful for immunosuppression while avoiding complications of Treg overactivation. Moreover, these results set the basis for further studies that might evaluate if a mAbCAR Treg–based approach could be suitable to ameliorate islet graft function and improve treatment of diabetes.

The basis for peripheral tolerance after transient mAbCAR induction in T cells is unclear. Since polyclonal Tregs may activate in response to specific allogeneic antigens and potentially become alloantigen specific, we speculate that mAbCAR stimulation may facilitate the formation of peripheral tolerance by somehow facilitating alloreactive Tregs, although further studies are required to assess this possibility.

We also observed that mAbCAR Treg–targeting luc^+ allogeneic pancreatic islets showed an unexpected and significant increase in BLI signal from the grafts that started in the very first days after transplant. Multiple cellular mechanisms could account for an improvement in this signal, including the possibility raised by others that the presence of a Treg-induced cytokine environment could promote both engraftment and islet β cell proliferation (42, 43). If so, this opens the exciting possibility that CAR Tregs could provide multiple signals to improve islet transplantation outcomes.

The use of mAbs to direct CAR T cells is an area of active investigation, and the approach could have a number of pitfalls. For example, FITC could be immunogenic in humans (44), thereby limiting use of mAbCAR targeting for clinical translation. If so, antibody-tagging systems (e.g., nanocapsules, DNA bridges, Fc-tagging sequences) that proved to be safe in different clinical applications could be adapted for overcoming this possible limitation. Moreover mAbCAR T cell activation via mAb could induce relevant side effects in the clinical setting (e.g., cytokine release syndrome). Our work demonstrates that in vitro preincubation of mAbCAR T cells with FITC mAb is feasible and effective in mouse models and that it may reduce the risk of such adverse events as early products of activation (e.g., inflammatory cytokines) are washed away before cell infusion. Studies in the human setting will help to understand the translational potential of this approach.

In summary, we describe a flexible, modular system for modifying CAR T cells that allows targeted homing to specific antigens and cells and activation of in vivo functions. In mice, this system was useful for targeting inflammation and achieving durable antigen-specific immune protection of tissues, including allografted pancreatic islets. Future uses of mAbCAR Treg strategies in humans could address persistent, urgent problems in clinical medicine needing targeted immunomodulation and preservation of tissue survival and function.

Methods

Mice. We performed experiments using gender-matched 8- to 16-week-old mice. BALB/c (H-2^d), C57BL/6 (H-2^b), and FVB/N (H-2^q) mice were purchased from Jackson Laboratories. *luc*$^+$ BALB/c mice were generated as described and were raised in the Stanford Animal Facility (45). C57BL/6 albino FoxP3 mutant mice expressing *luciferase* and *GFP* (FoxP3$^{luc/GFP}$) were a gift from Günter J. Hämmerling (German Cancer Research Center DKFZ, Heidelberg, Germany) and bred in our animal facility.

Cell isolation. For CD4$^+$ and/or CD8$^+$ T cells, we obtained cell suspensions from splenocytes and peripheral lymph node cells of donor animals, and we enriched them with anti-CD4 and/or anti-CD8 magnetic-activated cell sorting (MACS; Miltenyi Biotec).

For TCD BM, we flushed long bones by injecting PBS, after which we depleted T cells with anti-CD4 and anti-CD8 MACS beads.

For Tregs, we obtained pooled cell suspensions from spleens and lymph nodes, stained them for CD25-allophycocyanin (APC) (PC61, Biolegend) and CD4 (GK1.5 Biolegend), enriched them with anti-APC MACS beads, and sorted them for CD4$^+$CD25^{bright} cells or for CD4$^+$CD25$^+$GFP$^+$ cells from C57BL/6 albino FoxP3$^{luc/GFP}$ mice on a FACSAria or FACSAida (BD Biosciences). Purity of the final Treg product was always >95% CD4$^+$FoxP3$^+$ cells when using both the approaches.

Flow cytometric analysis and mass cytometry analysis. For flow cytometry, we purchased from Southern Biotech, BD Biosciences, eBioscience, R&D Systems, and Biolegend the following antibodies: CD4 (Biolegend, GK1.5), CD8 (Biolegend, 53-6.7), CD25 (Biolegend, PC61), FoxP3 (eBiosciences, FJK-16s), H-2D^d (Biolegend, 34-2-12), MAdCAM1 (Biolegend, MECA-367), CXCL12/SDF1 (R&D Systems, 79018), IgG1 (Southern Biotech, KLH/G2a-1-1), and IgG2a (BD, G155-178). We used the anti-mouse/rat FoxP3 Staining Set (eBioscience) for intranuclear Foxp3 staining and Fixable Viability Dye eFluor 506 (eBioscence) for dead cell staining. Analysis was performed on a LSR II (Becton Dickinson).

For mass cytometry, we used the antibody list as previously reported (46). For intranuclear factors, we used the anti-mouse/rat FoxP3 Staining Set (eBioscience) and for staining dead cells we use Cisplatin (Sigma-Aldrich). Analysis was performed on Cytof, and data were analyzed through Cytobank as previously described (47).

In vitro cell culture. Tregs or Tcons have been plated in 96-well or 48-well flat-bottom plates containing cRPMI, IL-2 (50 IU/ml for Tcons; 1,000 IU/ml for Tregs), and anti-CD3/CD28 beads (Dynabeads, Invitrogen, 1:10 bead/cell ratio for Tcons; 1:2 bead/cell ratio for Tregs). Tcons have been cultured for 2–4 days, washed, and then transfected. Tregs have been cultured for 18 consecutive days, checked every 6 days for purity by FACS analysis (CD4$^+$FoxP3$^+$ cells constantly > 90%), washed, and then transfected.

Transfection of T cells and Tregs and incubation with FITC-conjugated antibody. T cells and Tregs were transfected using MIRUS transfection reagents as per the manufacturer's protocol (Mirus Bio LLC). Briefly, cells were plated at a concentration of 5×10^5 cells/ml and were incubated with the 1X9Q DNA as well as the MIRUS reagent for 24–48 hours to allow for expression of the chimeric receptor. Transfected cells were then washed and incubated or not in vitro with the FITC-conjugated antibody of interest for 30 minutes on ice. FITC-conjugated antibodies that have been used for stimulation of mAbCAR T cells and/or mAbCAR Tregs are as follows: H-2D^d (34-2-12, Biolegend), MAdCAM1 (MECA-367, Biolegend), CXCL12/SDF1 (79018, R&D Systems), IgG1 (KLH/G2a-1-1, Southern Biotech), IgG2a (G155-178, BD Biosciences). Cells were then washed once more and injected into mice (0.5×10^6 to 1×10^6 cells/mouse)

Bone marrow transplantation, GvHD, and tumor models. For the mouse model of GvHD, BALB/c recipient mice were irradiated with 2 doses of 4-Gy total body irradiation 4 hours apart with 200-Kv X-ray source and rescued with 5×10^6 TCD BM cells from allogeneic C57BL/6 mice. GvHD was induced with 1×10^6 Tcons from C57BL/6 mice injected at day 0. Transplanted animals were kept in autoclaved cages with antibiotic water or antibiotic food (sulfamethoxazole-trimethoprim; Schein Pharmaceutical). C57BL/6 Tregs were injected at different time points and at different doses, as reported. For BLI analysis of cell proliferation *luc*$^+$ Tcons or Tregs have been used accordingly. In the tumor model with the A20 leukemia cell line, *luc*$^+$ 2×10^5/mouse A20 cells were injected together with TCD BM after lethal irradiation. Mice received different mAbCAR Tcon populations, as reported, and tumor growth was assessed in vivo by BLI. In vivo BLI was performed as described with an IVIS 29 charge-coupled device imaging system (Xenogen) (13). Images were analyzed with Living Image Software 4.3.1 (Xenogen). Mouse survival was reported, and mice were weighed weekly and the GvHD scores were calculated (48, 49).

Measurement of phosphorylation of STAT5. FACS-purified, in vitro–expanded, and transfected Tregs

were cultured overnight in complete RPMI without IL-2 supplementation. The cells were then washed in PBS (ThermoFisher). Phosphorylation of STAT5 was detected as described previously (47). Briefly, the cells were pulsed with 0, 100, 1,000, and 2,000 IU/ml recombinant IL-2 (rIL-2, Teceleukin, Hoffmann-La Roche) for 15 minutes before fixation with 4% paraformaldehyde (Sigma-Aldrich). Perm Buffer III from BD Biosciences was used for permeabilization. The following antibodies were used: Alexa Fluor 647–conjugated anti-STAT5 (pY694, BD Biosciences), Brilliant Violet 650–conjugated anti-CD4 (RM4-5, Biolegend), allophycocyanin cyanine 7–conjugated anti-CD25 (PC61, Biolegend), anti-FoxP3 (FSK-16s, Biolegend), phycoerythrin-conjugated anti-DYKDDDDK TAG (L5, Biolegend). Data were collected on a FACSAria (BD), and the data were analyzed using FlowJo Vx software (Treestar).

TCR repertoire sequencing and data processing. Total RNA was isolated from both transfected and untransfected Tregs with the Qiagen RNeasy Micro Kit. Rapid amplification of 5′ complementary DNA ends (5′RACE) was employed to capture VDJ genes of TCRβ. Briefly, first-strand cDNA was generated by Superscript II reverse transcriptase with oligo-dT30 (ThermoFisher) and a universal oligo was added to the 5′end of mRNAs (50). cDNA was then amplified with a TCRβ primer (5′-GGGTGGAGTCACATTTCTCAGATCCT) from a constant region and the 5′end universal primer (5′-AAGCAGTGGTATCAACGCAGAGT). The library was constructed with KAPA Hyper Prep Kits (Kapa Biosystems). The sequencing was carried out with a 500-cycle MiSeq Reagent Kit v2 on a illumina Miseq machine. After removing primer sequences, we used MiXCR (51) for VDJ rearrangement analysis and determined complementarity-determining region 3 (CDR3). CDR3 amino acid sequences and frequency were summarized from MiXCR outputs.

Mouse islet transplantation. For islet transplantation experiments, 100 mouse islets from 2- to 4-month-old donors aged were transplanted per recipient mouse. Islets were resuspended in cold Matrigel and transferred into the renal capsular space of host animals using a glass microcapillary tube. Transplant recipients were 2- to 4-month-old male mice and were anesthetized using ketamine/xylazine. Appropriate depth of anesthesia was confirmed by lack of toe-pinch response. After 2 weeks, kidneys with grafts were removed, fixed in 4% paraformaldehyde and processed for cryosectioning and immunohistology.

Immunostaining of islet transplant grafts. Primary antibodies used were guinea pig polyclonal anti-insulin (1:200, Dako, A0564), and secondary antibody used was donkey anti-guinea pig (1:500, Jackson Immunoresearch, 706-605-148). Samples were imaged using an SP2 confocal microscope with a ×40 objective.

Antigen specificity response after in vivo FITC-H-2D^d-mAbCAR Treg transfer. To analyze the antigen-specific response, mice received a secondary double skin graft MHC matched with the previously transplanted pancreatic graft (BALB/c) and "third-party" (FVB/N). All animals were anesthetized with ketamine/xylazine at 21 days after pancreatic islet transplantation. Under sterile conditions, MHC-matched and "third-party" skins (1 cm × 1 cm) were transplanted in dorsal site and sutured (4-0 Safil Violet, B. Braun). Buprenorphine (0.05 mg/Kg) was administered subcutaneously as analgesia before and after skin transplantation every 24 hours. Double skin graft survival was monitored in mice that received pancreatic islet graft and no Treg treatment (skin MHC matched with islet graft, skin "third party"), mice that received pancreatic islet graft and FITC-isotype-mAbCAR Tregs (skin MHC matched with islet graft, skin "third party"), and mice that received pancreatic islet graft and FITC-H-2D^d-mAbCAR Tregs (skin MHC matched with islet graft, skin "third party"). Signs of onset of rejection, such as dryness, loss of hair, contraction, scaling, and necrosis were recorded for a period of time of 21 days after transplantation. Grafts were considered rejected when necrosis and detachment of the graft was observed. At this point, the animals were euthanized, and histological analysis of skin grafts by hematoxylin and eosin and CD4 staining was performed.

Statistics. Log-rank test was used to detect differences in animal survival (Kaplan-Meier survival curves), while weight variation and GvHD score were analyzed with ANOVA test. All other comparisons were performed with the 2-tailed Student's t test. $P < 0.05$ was considered statistically significant.

Study approval. All animal experiments were performed in accordance with guidelines from the Stanford University Institutional Animal Care and Use Committee, and the study was approved by the Administrative Panel on Laboratory Animal Care, Stanford, California, USA.

Author contributions

Conception, experimental design, analysis, and interpretation were performed by AP, BPI, HP, MPC, and EHM. Experimental design was developed and analysis was performed by JB, KH, PPZ, TE, SWT, WS, and MA. Construct generation was performed by AR and XG. The manuscript was drafted for important intellectual content by AP, EHM, MPC, HP, BPI, RSN, and SKK. General supervision

was performed by EHM, AV, RSN, and SKK. All authors gave their agreement to be accountable for all aspects of the work in ensuring that questions related to the accuracy or integrity of any part of the work are appropriately investigated and resolved.

Address correspondence to: Everett Meyer, Division of Blood and Marrow Transplantation, Department of Medicine, Stanford University School of Medicine, 269 West Campus Drive, CCSR Building Room 2245C, Stanford, CA 94305-5623, USA. Phone: 650.725.5816; Email: evmeyer@stanford.edu. Or to: Antonio Pierini, Department of Medicine, Hematopoietic Stem Cell Transplantation Program, University of Perugia, CREO, Piazzale Menghini, Perugia, 06132, Italy. Phone: 390755783157; Email: antonio.pierini@unipg.it.

EHM's present address is: Division of Blood and Marrow Transplantation, Department of Medicine, Stanford University School of Medicine, Stanford, California, USA.

1. Maus MV, June CH. Making better chimeric antigen receptors for adoptive t-cell therapy. *Clin Cancer Res*. 2016;22(8):1875–1884.
2. Barrett DM, Grupp SA, June CH. Chimeric antigen receptor- and TCR-modified T cells enter main street and Wall Street. *J Immunol*. 2015;195(3):755–761.
3. Sadelain M. Chimeric antigen receptors: driving immunology towards synthetic biology. *Curr Opin Immunol*. 2016;41:68–76.
4. Brunstein CG, et al. Infusion of ex vivo expanded T regulatory cells in adults transplanted with umbilical cord blood: safety profile and detection kinetics. *Blood*. 2011;117(3):1061–1070.
5. Morris EC, Stauss HJ. Optimizing T-cell receptor gene therapy for hematologic malignancies. *Blood*. 2016;127(26):3305–3311.
6. Park JH, Geyer MB, Brentjens RJ. CD19-targeted CAR T-cell therapeutics for hematologic malignancies: interpreting clinical outcomes to date. *Blood*. 2016;127(26):3312–3320.
7. Garfall AL, Stadtmauer EA, June CH. Chimeric antigen receptor T cells in myeloma. *N Engl J Med*. 2016;374(2):194.
8. Ruella M, June CH. Chimeric antigen receptor T cells for B cell neoplasms: choose the right CAR for you. *Curr Hematol Malig Rep*. 2016;11(5):368–384.
9. Gill S, June CH. Going viral: chimeric antigen receptor T-cell therapy for hematological malignancies. *Immunol Rev*. 2015;263(1):68–89.
10. Porter DL, Levine BL, Kalos M, Bagg A, June CH. Chimeric antigen receptor-modified T cells in chronic lymphoid leukemia. *N Engl J Med*. 2011;365(8):725–733.
11. Fedorov VD, Themeli M, Sadelain M. PD-1- and CTLA-4-based inhibitory chimeric antigen receptors (iCARs) divert off-target immunotherapy responses. *Sci Transl Med*. 2013;5(215):215ra172.
12. Edinger M. Driving allotolerance: CAR-expressing Tregs for tolerance induction in organ and stem cell transplantation. *J Clin Invest*. 2016;126(4):1248–1250.
13. MacDonald KG, et al. Alloantigen-specific regulatory T cells generated with a chimeric antigen receptor. *J Clin Invest*. 2016;126(4):1413–1424.
14. Nishikawa H, Sakaguchi S. Regulatory T cells in cancer immunotherapy. *Curr Opin Immunol*. 2014;27:1–7.
15. Plitas G, Rudensky AY. Regulatory T cells: differentiation and function. *Cancer Immunol Res*. 2016;4(9):721–725.
16. Di Ianni M, et al. Tregs prevent GVHD and promote immune reconstitution in HLA-haploidentical transplantation. *Blood*. 2011;117(14):3921–3928.
17. Edinger M, Cao YA, Verneris MR, Bachmann MH, Contag CH, Negrin RS. Revealing lymphoma growth and the efficacy of immune cell therapies using in vivo bioluminescence imaging. *Blood*. 2003;101(2):640–648.
18. Schneidawind D, Pierini A, Negrin RS. Regulatory T cells and natural killer T cells for modulation of GVHD following allogeneic hematopoietic cell transplantation. *Blood*. 2013;122(18):3116–3121.
19. Pierini A, Schneidawind D, Nishikii H, Negrin RS. Regulatory T cell immunotherapy in immune-mediated diseases. *Curr Stem Cell Rep*. 2015;1(4):177–186.
20. Martelli MF, et al. HLA-haploidentical transplantation with regulatory and conventional T-cell adoptive immunotherapy prevents acute leukemia relapse. *Blood*. 2014;124(4):638–644.
21. Josefowicz SZ, Lu LF, Rudensky AY. Regulatory T cells: mechanisms of differentiation and function. *Annu Rev Immunol*. 2012;30:531–564.
22. Ohkura N, Kitagawa Y, Sakaguchi S. Development and maintenance of regulatory T cells. *Immunity*. 2013;38(3):414–423.
23. Sakaguchi S, Vignali DA, Rudensky AY, Niec RE, Waldmann H. The plasticity and stability of regulatory T cells. *Nat Rev Immunol*. 2013;13(6):461–467.
24. Mikami N, Sakaguchi S. CD28 signals the differential control of regulatory T cells and effector T cells. *Eur J Immunol*. 2014;44(4):955–957.

25. Abken H. Costimulation engages the gear in driving CARs. *Immunity*. 2016;44(2):214–216.

26. Kawalekar OU, et al. Distinct signaling of coreceptors regulates specific metabolism pathways and impacts memory development in CAR T cells. *Immunity*. 2016;44(2):380–390.

27. Yoon J, Schmidt A, Zhang AH, Königs C, Kim YC, Scott DW. FVIII-specific human chimeric antigen receptor T-regulatory cells suppress T- and B-cell responses to FVIII. *Blood*. 2017;129(2):238–245.

28. Anchang B, et al. Visualization and cellular hierarchy inference of single-cell data using SPADE. *Nat Protoc*. 2016;11(7):1264–1279.

29. Gorfu G, Rivera-Nieves J, Ley K. Role of beta7 integrins in intestinal lymphocyte homing and retention. *Curr Mol Med*. 2009;9(7):836–850.

30. Kraal G, Schornagel K, Streeter PR, Holzmann B, Butcher EC. Expression of the mucosal vascular addressin, MAdCAM-1, on sinus-lining cells in the spleen. *Am J Pathol*. 1995;147(3):763–771.

31. Noyan F, et al. Prevention of allograft rejection by use of regulatory T cells with an MHC-specific chimeric antigen receptor. *Am J Transplant*. 2017;17(4):917–930.

32. Boardman DA, et al. Expression of a chimeric antigen receptor specific for donor HLA class I enhances the potency of human regulatory T cells in preventing human skin transplant rejection. *Am J Transplant*. 2017;17(4):931–943.

33. Tamada K, et al. Redirecting gene-modified T cells toward various cancer types using tagged antibodies. *Clin Cancer Res*. 2012;18(23):6436–6445.

34. Ma JS, et al. Versatile strategy for controlling the specificity and activity of engineered T cells. *Proc Natl Acad Sci USA*. 2016;113(4):E450–E458.

35. Beilhack A, et al. Prevention of acute graft-versus-host disease by blocking T-cell entry to secondary lymphoid organs. *Blood*. 2008;111(5):2919–2928.

36. Beilhack A, et al. In vivo analyses of early events in acute graft-versus-host disease reveal sequential infiltration of T-cell subsets. *Blood*. 2005;106(3):1113–1122.

37. Veerapathran A, et al. Human regulatory T cells against minor histocompatibility antigens: ex vivo expansion for prevention of graft-versus-host disease. *Blood*. 2013;122(13):2251–2261.

38. Veerapathran A, Pidala J, Beato F, Yu XZ, Anasetti C. Ex vivo expansion of human Tregs specific for alloantigens presented directly or indirectly. *Blood*. 2011;118(20):5671–5680.

39. Brennan PJ, Brigl M, Brenner MB. Invariant natural killer T cells: an innate activation scheme linked to diverse effector functions. *Nat Rev Immunol*. 2013;13(2):101–117.

40. Gagliani N, et al. Coexpression of CD49b and LAG-3 identifies human and mouse T regulatory type 1 cells. *Nat Med*. 2013;19(6):739–746.

41. Zhang M, et al. The impact of Nucleofection® on the activation state of primary human CD4 T cells. *J Immunol Methods*. 2014;408:123–131.

42. Dirice E, et al. Soluble factors secreted by T cells promote β-cell proliferation. *Diabetes*. 2014;63(1):188–202.

43. Russell MA, Morgan NG. The impact of anti-inflammatory cytokines on the pancreatic β-cell. *Islets*. 2014;6(3):e950547.

44. Ha SO, Kim DY, Sohn CH, Lim KS. Anaphylaxis caused by intravenous fluorescein: clinical characteristics and review of literature. *Intern Emerg Med*. 2014;9(3):325–330.

45. Cao YA, et al. Shifting foci of hematopoiesis during reconstitution from single stem cells. *Proc Natl Acad Sci USA*. 2004;101(1):221–226.

46. Murai M, et al. Peyer's patch is the essential site in initiating murine acute and lethal graft-versus-host reaction. *Nat Immunol*. 2003;4(2):154–160.

47. Kim BS, et al. Treatment with agonistic DR3 antibody results in expansion of donor Tregs and reduced graft-versus-host disease. *Blood*. 2015;126(4):546–557.

48. Cooke KR, et al. An experimental model of idiopathic pneumonia syndrome after bone marrow transplantation: I. The roles of minor H antigens and endotoxin. *Blood*. 1996;88(8):3230–3239.

49. Ueha S, et al. Intervention of MAdCAM-1 or fractalkine alleviates graft-versus-host reaction associated intestinal injury while preserving graft-versus-tumor effects. *J Leukoc Biol*. 2007;81(1):176–185.

50. Picelli S, Faridani OR, Björklund AK, Winberg G, Sagasser S, Sandberg R. Full-length RNA-seq from single cells using Smart-seq2. *Nat Protoc*. 2014;9(1):171–181.

51. Bolotin DA, et al. MiXCR: software for comprehensive adaptive immunity profiling. *Nat Methods*. 2015;12(5):380–381.